PHYSICAL REVIEW B **83**, 060512(R) (2011)

Superconductivity at 32 K in single-crystalline $Rb_xFe_{2-y}Se_2$

A. F. Wang, J. J. Ying, Y. J. Yan, R. H. Liu, X. G. Luo,* Z. Y. Li, X. F. Wang, M. Zhang, G. J. Ye, P. Cheng, Z. J. Xiang, and X. H. Chen†

Hefei National Laboratory for Physical Science at Microscale and Department of Physics, University of Science and Technology of China, Hefei, Anhui 230026, People's Republic of China

(Received 26 December 2010; revised manuscript received 29 January 2011; published 28 February 2011)

We successfully grew the high-quality single crystal of $Rb_{0.88}Fe_{1.81}Se_2$, which shows a clear superconducting transition in magnetic susceptibility and electrical resistivity. Resistivity shows the onset superconducting transition T_c at 32.1 K and zero resistivity at 30 K. From the low-temperature iso-magnetic-field magnetoresistance, the large upper critical field $H_{c2}(0)$ has been estimated to be as high as 180 T for the field applied within the *ab* plane and 59 T for the field applied along the *c* axis. The anisotropy $H_{c2}^{ab}(0)/H_{c2}^{c}(0)$ is around 3.0, lying right between those observed in $K_xFe_2Se_2$ and $Cs_xFe_2Se_2$.

DOI: 10.1103/PhysRevB.83.060512 PACS number(s): 74.70.Xa, 75.30.Gw, 72.15.−v

The newly discovered iron-based superconductors have attracted worldwide attention in the past three years[1–5] because of their high superconducting transition temperature (T_c as high as 55 K) and the fact that superconductivity emerges in proximity to the magnetically ordered state.[6,7] The fact that superconductivity in the iron-pnictide compounds is closely related to the magnetic correlations inspires researchers tending to connect them with the high-T_c cuprates, in which superconductivity is realized by suppressing the antiferromagnetic Mott-insulating state. It is helpful to understand the superconducting mechanism in the same theoretical scenario for both families. Up to now, a variety of Fe-based superconductors, such as the ZrCuSiAs-type *Ln*FeAsO (*Ln*-1111, *Ln* is a rare-earth element),[1–3] the $ThCr_2Si_2$-type $AeFe_2As_2$ (*Ae*-122, *Ae* is an alkaline-earth element),[4] the Fe_2As-type *A*FeAs (*A*-111, *A* is Li or Na),[8–10] and the anti-PbO-type Fe(Se,Te) (11),[11] have been discovered. Antiferromagnetic spin density wave instability usually exists in the parent compound of the superconducting *Ln*-1111 and *Ae*-122, and even coexists with superconductivity in the slightly doping levels of *Ln*-1111, *Ae*-122, and *A*-111. While for the 11 phase, magnetism is quite complicated and its relationship to superconductivity remains more unrecognized.

All of the above-mentioned Fe-based superconductors have a common structural feature with the edge-sharing $FeAs_4$ ($FeSe_4$) tetrahedra formed FeAs (FeSe) layers. The superconductivity in these compounds is thought to be intimately associated with the height of the anion from the Fe layer.[12] The FeAs-based compounds usually possess cations or building blocks between the FeAs layers, while the Fe(Se,Te) family has an extremely simple structure with only the FeSe layers stacking along the *c* axis without other cations between them.[11] High pressure has been used to change the height of the anion from the Fe layer in Fe(Se,Te). Especially, T_c can reach 37 K (onset) under 4.5 GPa from 8 K in FeSe (Ref. 13) with a pressure-dependent ratio of T_c as large as $dT_c/dP \sim 9.1$ K/GPa, which is the highest pressure effect among all the Fe-based superconductors.[13] Researchers attempted to intercalate Tl between the FeSe layers to change the local structure of the FeSe family. However, an antiferromagnetic ordering formed at temperatures as high as 450 K,[14] and no superconductivity was observed in $TlFe_2Se_2$. Very recently, the alkali atoms K and Cs were successfully intercalated between the FeSe layers, and superconductivity was enhanced from $T_c = 8$ K of the pure FeSe to 30 K and 27 K (onset) without any external pressure.[15–18] This indicates that T_c in the FeSe family can really be enhanced by intercalating cations between the FeSe layers.

In this article, we successfully grew the single crystals of a new superconductor $Rb_xFe_2Se_2$ by using the Bridgeman method. The crystals showed an onset T_c of 32.1 K and zero resistivity at about 30 K. Nearly 100% superconducting volume fraction was observed through the zero-field-cooling (ZFC) magnetic susceptibility measurements. The upper critical field $H_{c2}(0)$ was estimated from the iso-magnetic-field magnetoresistance as high as 180 T with the field applied within the *ab* plane and 59 T with the field applied along the *c* axis.

Single crystals of $Rb_xFe_2Se_2$ were grown by the Bridgeman method. The starting material FeSe was obtained by reacting the Fe powder with Se powder with Fe:Se = 1:1 at 700 °C for 4 h. Rb pieces and FeSe powder were put into a small quartz tube with the nominal composition of $Rb_{0.8}Fe_2Se_2$. Due to the high activity of the Rb metal, the single-wall quartz tube would have been corrupted and broken during the growth procedure. Therefore, the double-wall quartz tube was used here. A small quartz tube was sealed under a high vacuum and then placed into a bigger quartz tube. Subsequently, the bigger quartz tube was evacuated and sealed. The mixture was heated to 980 °C in 10 h and kept for 4 h, and then melted at 1080 °C for 2 h, and later slowly cooled down to 780 °C at a rate of 6 °C/h. After that, the temperature was cooled down to room temperature by shutting down the furnace. The obtained rod on the bottom of the inner tube was then removed from the silica tubes in the glove box. All the products are single crystals and no obvious other phase can be observed. The obtained single crystals show a flat shiny surface with a dark black color. The crystals are easy to cleave, and thin crystals with thickness less than 100 μm can be easily obtained.

The single crystals were characterized by x-ray diffraction (XRD), energy dispersive x-ray (EDX) spectroscopy, inductively coupled plasma atomic emission spectroscopy (ICP-AES), magnetic susceptibility, and electrical transport measurements. Powder XRD and single-crystal XRD were

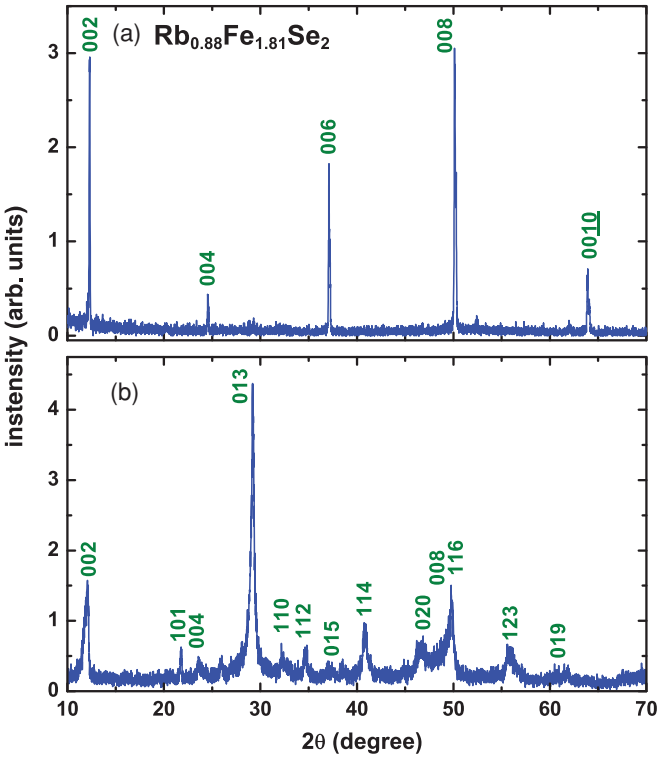

FIG. 1. (Color online) X-ray diffraction patterns for $Rb_{0.88}Fe_{1.81}Se_2$. (a) Single-crystal XRD pattern; (b) XRD pattern of the powdered $Rb_{0.88}Fe_{1.81}Se_2$.

performed on the theta/theta rotating anode x-ray (TTRAX3) diffractometer with Cu $K\alpha$ radiation and a fixed graphite monochromator. Magnetic susceptibility measurements were carried out using the Quantum Design magnetic property measurement system (MPMS) superconducting quantum interference device (SQUID). The measurement of resistivity and magnetoresistance were done on the Quantum Design physical property measurement system (PPMS-9).

Figure 1 shows the single-crystal XRD [Fig. 1(a)] and powder XRD [Fig. 1(b)] after grinding the single crystals into powder. Only (00l) reflections were recognized in Fig. 1(a), indicating that the crystals of $Rb_xFe_2Se_2$ were perfectly grown along the c axis. From the powder XRD patterns in Fig. 1(b), the lattice constants were calculated based on the symmetry I4/mmm with the lattice parameters a = 3.925 Å; and c = 14.5655 Å. The lattice constants of a and c lie between those of $K_xFe_2Se_2$ and $Cs_xFe_2Se_2$, respectively. It is consistent with the expectation based on the variation of the radii of the K, Rb, and Cs ions (K 1.51 Å, Rb 1.63 Å, Cs 1.78 Å).[19] The elemental analysis of the crystals were performed by the EDX and ICP-AES. The EDX results for five points show the standard deviations of 0.034 for Rb and 0.027 for Se, indicating the composition of the crystal is homogeneous. As we know, however, EDX is quite qualitative and has large errors sometimes. Therefore, we use a more accurate method, ICP-AES, to determine the actual composition of the crystal. The ICP-AES gives Rb:Fe:Se to be 0.88:1.81:2, which is consistent with the cases of $K_xFe_2Se_2$ and $Cs_xFe_2Se_2$.[15,17] We will use this proportion of Rb, Fe, and Se in the formula of the compound in the following text.

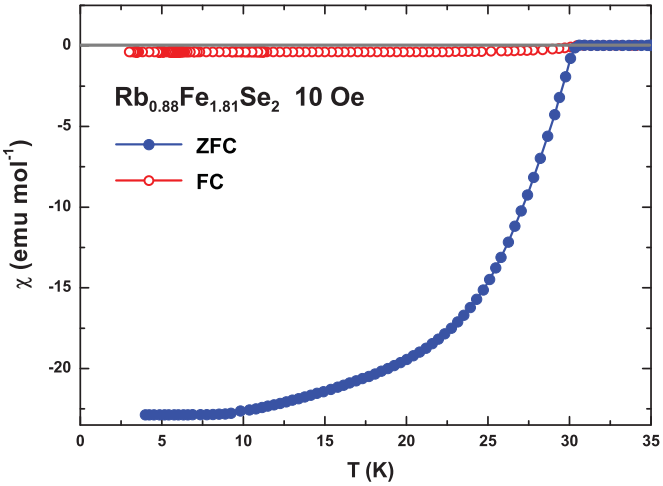

FIG. 2. (Color online) Temperature dependence of the zero-field cooling and field cooling susceptibility taken at 10 Oe with the magnetic field parallel to the *ab* plane for the single-crystalline $Rb_{0.88}Fe_{1.81}Se_2$.

Figure 2 shows magnetic susceptibility as a function of temperature below 35 K for the single-crystalline $Rb_{0.88}Fe_{1.81}Se_2$ under a magnetic field of 10 Oe. The zero-field-cooling (ZFC) and field cooling (FC) susceptibilities show that the superconducting shield begins to emerge at about 30.6 K and then show a clear transition. The ZFC magnetic susceptibility becomes saturating below 10 K, indicating the high quality of the single crystal. The superconducting volume fraction estimated from the ZFC magnetization at 4 K is 100%. All of these demonstrate a bulk superconductivity nature in the $Rb_{0.88}Fe_{1.81}Se_2$ single crystals.

Figure 3 shows the magnetic susceptibility of $Rb_{0.88}Fe_{1.81}Se_2$ with the magnetic field of 5 T applied parallel and perpendicular to the c axis from 10 to 400 K. At low temperature, the superconducting trace can still be found because of a drop in susceptibility. When the magnetic field is applied along the c axis, the magnetic susceptibility gradually decreases with decreasing the temperature. The susceptibility shows a minimum at about 120 K with the magnetic field

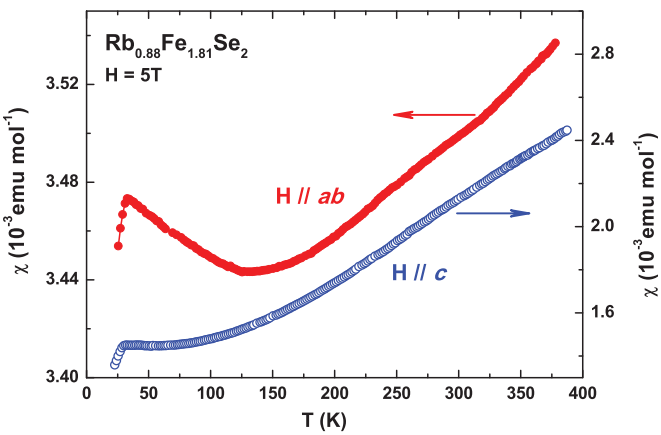

FIG. 3. (Color online) Magnetic susceptibility at 5 T for the single-crystalline $Rb_{0.88}Fe_{1.81}Se_2$ with the magnetic field along and perpendicular to the c axis.

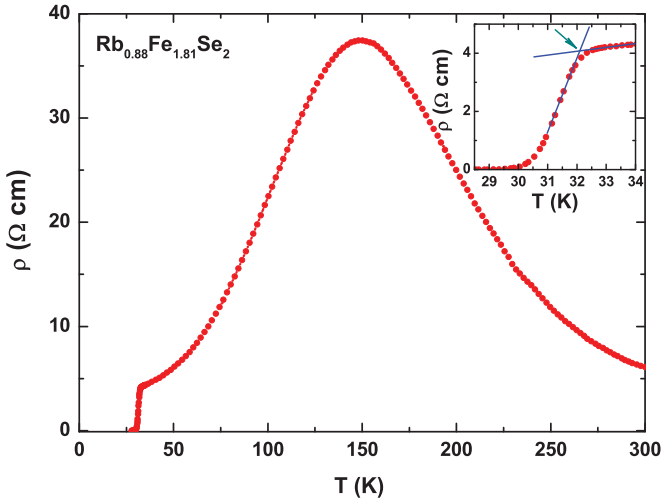

FIG. 4. (Color online) Temperature dependence of resistivity for th single-crystalline $Rb_{0.88}Fe_{1.81}Se_2$. The inset is the zoom plot of resistivity around the superconducting transition.

applied within the *ab* plane. Above 120 K, the susceptibility monotonically increases with increasing temperature; while it gradually increases with decreasing temperature down to about 40 K just above the superconducting transition temperature. Although the in-plane $\chi(T)$ shows a minimum 120 K above T_c, the magnitude of the susceptibility only changes by less than 2.5% in the temperature range from 40 to 400 K. Such behavior of the susceptibility in $Rb_{0.88}Fe_{1.81}Se_2$ is exactly the same as that observed in $Cs_{0.86}Fe_{1.66}Se_2$.[18] Therefore, such peculiar behavior of susceptibility is a common feature. The continuous decrease of the susceptibility with decreasing the temperature suggests a strong antiferromagnetic spin fluctuation. Such spin fluctuation could be related to the superconductivity.

Figure 4 shows the in-plane resistivity as the function of the temperature for the single-crystalline $Rb_{0.88}Fe_{1.81}Se_2$. The $Rb_{0.88}Fe_{1.81}Se_2$ shows a semiconductor-like behavior at high temperature, and displays a maximum resistivity at about 150 K followed by a metallic behavior below 150 K and then a superconducting transition at about 32 K. A similar resistivity has been observed in $K_xFe_2Se_2$.[15,18] It seems that the resistivity behavior observed here is a common feature. The temperature corresponding to the maximum resistivity in $Rb_{0.88}Fe_{1.81}Se_2$ is higher than that for $K_xFe_2Se_2$ reported by Guo *et al.* (around 100 K)[15] and by Ying *et al.* (around 120 K),[18] while it is less than that reported by Mizuguchi *et al.* (∼200 K).[16] The maximum resistivity in the $Rb_{0.88}Fe_{1.81}Se_2$ crystal here (∼37 Ω cm) is much larger than that of $K_xFe_2Se_2$ in the previous report (∼3 Ω cm).[16] The temperature of the maximum resistivity strongly depends on the sample. The different temperature of the maximum resistivity could arise from the vacancies within the FeSe layers. The residual resistance ratio between 150 and 33 K is as large as 9. With further decreasing of the temperature, superconductivity emerges at about 32.1 K and resistivity reaches zero at about 30 K. These values are very close to those observed in $K_xFe_2Se_2$.[15,16] The resistivity of the $Rb_{0.88}Fe_{1.81}Se_2$ crystal is 6 Ω cm at room temperature, which is much larger than those of the FeSe single crystals[20] and the

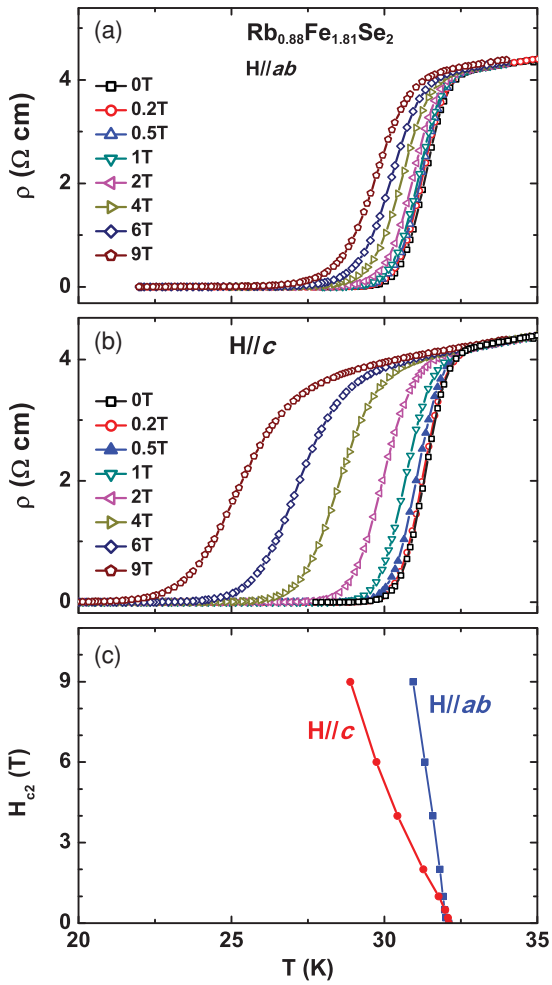

FIG. 5. (Color online) (a) and (b) show the temperature dependence of resistivity for the single-crystalline $Rb_{0.88}Fe_{1.81}Se_2$ with the magnetic field parallel and perpendicular to the *ab* plane, respectively; (c) temperature dependence of the upper critical field $H_{c2}(T)$ for the $Rb_{0.88}Fe_{1.81}Se_2$ crystal.

other iron-pnictide superconductors.[21] This may arise from the large disorder induced by deficiencies with the conducting FeSe layers. The occurrence of superconductivity in a system with so high a resistivity demands further theoretical and experimental investigations.

Resistivity as a function of temperature under the magnetic fields applied in *ab* plane and along the *c* axis is shown in Figs. 5(a) and 5(b). The transition temperature of superconductivity is suppressed gradually, and the transition is broadened with increasing the magnetic field. An obvious difference in the effect of the magnetic field along different directions on the superconductivity can be observed. To study this difference clearly, we defined the T_c as the temperature where the resistivity exhibited a 90% drop right above the superconducting transition. The anisotropic $H_{c2}(T)$ is shown in Fig. 5(c) for the two field directions, respectively. Within the weak-coupling BCS theory, the upper critical field at $T = 0$ K can be determined by the Werthamer-Helfand-Hohenberg (WHH) equation[22] $H_{c2}(0) = 0.693[-(dH_{c2}/dT)]_{T_c}T_c$. From Fig. 5(c), we can have $[-(dH_{c2}^{ab}/dT)]_{T_c} = 8.09$ T/K, $[-(dH_{c2}^{c}/dT)]_{T_c} = 2.66$ T/K

and $T_c = 32.1$ K. Then the $H_{c2}(0)$ can be estimated to be 180 and 59 T with the magnetic field applied within the *ab* plane and along the *c* axis, respectively. These values are less than those in $K_xFe_2Se_2$,[16,18] while larger than those in $CsFe_2Se_2$.[18] The anisotropy $H_{c2}^{ab}(0)/H_{c2}^{c}(0)$ is about 3.0, and this value just lies right between those of $K_xFe_2Se_2$ and $Cs_xFe_2Se_2$. This anisotropy value is similar to 2.5–3.5 in the Sn-flux grown $Ba_{0.55}K_{0.45}Fe_2As_2$ crystal,[23,24] but larger than 1.70∼1.86 in the FeAs-flux grown $Ba_{0.60}K_{0.40}Fe_2As_2$ crystal[25] and less than 4∼6 in the F-doped NdFeAsO crystal.[26]

We have systematically grown the single crystals $A_xFe_2Se_2$ (A = K, Rb, and Cs). A maximum resistivity as shown in Fig. 4 is widely observed in $K_xFe_2As_2$ (Refs. 15, 16, and 18) and $Rb_xFe_2As_2$. The very large magnitude of resistivity has been observed for all the $A_xFe_2Se_2$ single crystals, with the superconductivity still existing. This implies that there is a large amount of deficiencies, with the conducting FeSe layers inducing a very high resistivity. However, superconductivity could be less influenced by such deficiencies because of the coexistence of high resistivity and superconductivity. Further study on the origin of the deficiencies should be conducted to understand the normal-state behavior, even the superconductivity of $A_xFe_2Se_2$ materials.

In conclusion, we successfully grew superconductor $Rb_{0.88}Fe_{1.81}Se_2$ single crystals. T_c^{onset} is 32.1 K determined by resistivity measurement, and zero resistivity is reached at 30 K. The ZFC dc magnetic susceptibility indicates that the crystal is fully diamagnetic. A large $H_{c2}(0)$ is observed, which is similar to those in the iron-pnictide superconductors.[24,27] The anisotropy $H_{c2}^{ab}(0)/H_{c2}^{c}(0)$ is 3.0, lying right between those of $K_xFe_2Se_2$ and $Cs_xFe_2Se_2$. A common peculiar susceptibility in the normal state is observed in $Rb_{0.88}Fe_{1.81}Se_2$.

This work is supported by the Natural Science Foundation of China, Ministry of Science and Technology of China, and Chinese Academy of Sciences.

*xgluo@mail.ustc.edu.cn

†chenxh@ustc.edu.cn

[1] Yoichi Kamihara, Takumi Watanabe, Masahiro Hirano, and Hideo Hosono, J. Am. Chem. Soc. **130**, 3296 (2008).

[2] X. H. Chen, T. Wu, G. Wu, R. H. Liu, H. Chen, and D. F. Fang, Nature (London) **453**, 761 (2008).

[3] Z. A. Ren, W. Lu, J. Yang, W. Yi, X. L. Shen, Z. C. Li, G. C. Che, X. L. Dong, L. L. Sun, F. Zhou, and Z. X. Zhao, Chin. Phys. Lett. **25**, 2215 (2008).

[4] M. Rotter, M. Tegel, and D. Johrendt, Phys. Rev. Lett. **101**, 107006 (2008).

[5] R. H. Liu, G. Wu, T. Wu, D. F. Fang, H. Chen, S. Y. Li, K. Liu, Y. L. Xie, X. F. Wang, R. L. Yang, L. Ding, C. He, D. L. Feng, and X. H. Chen, Phys. Rev. Lett. **101**, 087001 (2008).

[6] H. Chen, Y. Ren, Y. Qiu, Wei Bao, R. H. Liu, G. Wu, T. Wu, Y. L. Xie, X. F. Wang, Q. Huang, and X. H. Chen, Europhys. Lett. **85**, 17006 (2009).

[7] Clarina de la Cruz, Q. Huang, J. W. Lynn, Jiying Li, W. Ratcliff II, J. L. Zarestky, H. A. Mook, G. F. Chen, J. L. Luo, N. L. Wang, and Pengcheng Dai, Nature (London) **453**, 899 (2008).

[8] X. C. Wang, Q. Q. Liu, Y. X. Lv, W. B. Gao, L. X. Yang, R. C. Yu, F. Y. Li, and C. Q. Jin, Solid State Commun. **148**, 538 (2008).

[9] J. H. Tapp, Z. Tang, B. Lv, K. Sasmal, B. Lorenz, Paul C. W. Chu, and A. M. Guloy, Phys. Rev. B **78**, 060505(R) (2008).

[10] D. R. Parker, M. J. Pitcher, P. J. Baker, I. Franke, T. Lancaster, S. J. Blundell, and S. J. Clarke, Chem. Commun. (Cambridge) **2009**, 2189.

[11] F. C. Hsu, J. Y. Luo, K. W. The, T. K. Chen, T. W. Huang, P. M. Wu, Y. C. Lee, Y. L. Huang, Y. Y. Chu, D. C. Yan, and M. K. Wu, Proc. Nat. Acad. Sci. **105**, 14262 (2008).

[12] Y. Mizuguchi, Y. Hara, K. Deguchi, S. Tsuda, T. Yamaguchi, K. Takeda, H. Kotegawa, H. Tou, and Y. Takano, Supercond. Sci. Technol. **23**, 054013 (2010).

[13] S. Medvedev, T. M. McQueen, I. Trojan, T. Palasyuk, M. I. Eremets, R. J. Cava, S. Naghavi, F. Casper, V. Ksenofontov, G. Wortmann, and C. Felser, Nat. Mater. **8**, 630 (2009).

[14] J. J. Ying, A. F. Wang, Z. J. Xiang, X. G. Luo, R. H. Liu, X. F. Wang, Y. J. Yan, M. Zhang, G. J. Ye, P. Cheng, and X. H. Chen, e-print arXiv:1012.2929.

[15] J. Guo, S. Jin, G. Wang, S. Wang, K. Zhu, T. Zhou, M. He, and X. Chen, Phys. Rev. B **82**, 180520 (2010).

[16] Yoshikazu Mizuguchi, Hiroyuki Takeya, Yasuna Kawasaki, Toshinori Ozaki, Shunsuke Tsuda, Takahide Yamaguchi, and Yoshihiko Takano, Appl. Phys. Lett. **98**, 042511 (2011).

[17] A. Krzton-Maziopa, Z. Shermadini, E. Pomjakushina, V. Pomjakushin, M. Bendele, A. Amato, R. Khasanov, H. Luetkens, and K. Conder, J. Phys. Condens. Matter **23**, 052203 (2011).

[18] J. J. Ying, X. F. Wang, X. G. Luo, A. F. Wang, M. Zhang, Y. J. Yan, Z. J. Xiang, R. H. Liu, P. Cheng, G. J. Ye, and X. H. Chen, e-print arXiv:1012.5552.

[19] R. D. Shannon, Acta Crystallogr. Sect. A **32**, 751 (1976).

[20] D. Braithwaite, B. Salce, G. Lapertot, F. Bourdarot, C. Marin, D. Aoki, and M. Hanfland, J. Phys. Condens. Matter **21**, 232202 (2009).

[21] X. F. Wang, T. Wu, G. Wu, R. H. Liu, H. Chen, Y. L. Xie, and X. H. Chen, New J. Phys. **11**, 045003 (2009).

[22] N. R. Werthamer, E. Helfand, and P. C. Hohenberg, Phys. Rev. **147**, 295 (1966).

[23] N. Ni, S. L. Budko, A. Kreyssig, S. Nandi, G. E. Rustan, A. I. Goldman, S. Gupta, J. D. Corbett, A. Kracher, and P. C. Canfield, Phys. Rev. B **78**, 014507 (2008).

[24] M. M. Altarawneh, K. Collar, C. H. Mielke, N. Ni, S. L. Budko, and P. C. Canfield, Phys. Rev. B **87**, 220505 (2008).

[25] Z. S. Wang, H. Q. Luo, C. Ren, and H. H. Wen, Phy. Rev. B **78**, 140501(R) (2008).

[26] Y. Jia, P. Cheng, L. Fang, H. Luo, H. Yang, C. Ren, L. Shan, C. Z. Gu, and H. H. Wen, Appl. Phys. Lett. **93**, 032503 (2008).

[27] H. Q. Yuan, J. Singleton, F. F. Balakirev, S. A. Baily, G. F. Chen, J. L. Luo, and N. L. Wang, Nature (London) **457**, 565 (2009).